

## $f_2$ , $\sigma$ , AND $2\pi$ EXCHANGES IN $\rho$ MESON PHOTOPRODUCTION

YONGSEOK OH

*Institute of Physics and Applied Physics, Yonsei University,  
Seoul 120-749, Korea*

*E-mail: yoh@phya.yonsei.ac.kr*

T.-S. H. LEE

*Physics Division, Argonne National Laboratory, Argonne, Illinois 60439, U.S.A.*

*E-mail: lee@theory.phy.anl.gov*

The  $\sigma$  meson exchange model for  $\rho$  photoproduction at low energies is re-examined and a new model is developed by considering explicit two-pion exchange and the  $f_2$  tensor meson exchange. The  $f_2$  exchange model, which is motivated by the low energy proton-proton elastic scattering, is constructed by fully taking into account of the tensor structure of the  $f_2$  meson interactions. Phenomenological informations together with tensor meson dominance and vector meson dominance assumptions are used to estimate the  $f_2$  meson's coupling constants. For  $2\pi$  exchange, the loop terms including intermediate  $\pi N$  and  $\omega N$  channels are calculated using the coupling constants determined from the study of pion photoproduction. It is found that our model with  $f_2$  and  $2\pi$  exchanges can successfully replace the commonly used  $\sigma$  exchange model that suffers from the big uncertainty of the coupling constants. We found that the two models can be distinguished by examining the single and double spin asymmetries.

Recently the measurements on the electromagnetic production of vector mesons from the nucleon targets have been reported from the CLAS of TJNAF<sup>1-3</sup>, GRAAL of Grenoble<sup>4</sup>, and LEPS of SPring-8<sup>5,6</sup>. More data with high accuracy on various physical quantities of these processes are expected to come soon. These new data replace the limited old data of low statistics and provide an opportunity to understand the production mechanism of vector mesons at low energies. They are also expected to shed light on resolving the 'missing resonance' problem<sup>7-10</sup>.

However, it is well-known that thorough understanding of the nonresonant background mechanisms is crucial to extract the properties of the resonances and to identify any missing resonances from the data for meson

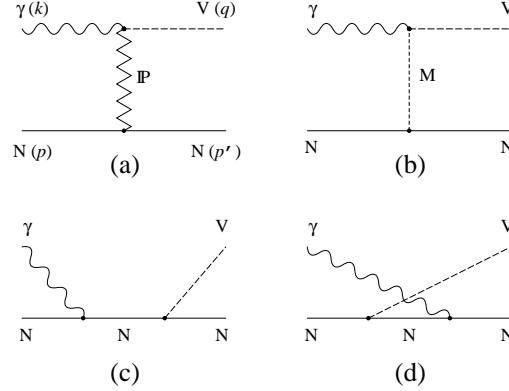


Figure 1. Models for  $\rho$  photoproduction. (a,b)  $t$ -channel Pomeron and one-meson exchanges ( $M = f_2, \pi, \eta, \sigma$ ). (c,d)  $s$ - and  $u$ -channel nucleon pole terms.

production processes<sup>11,12</sup>. As a continuation of our effort in this direction<sup>8,11</sup>, we explore the nonresonant mechanisms of  $\rho$  photoproduction in this work.

Through the analyses of vector meson photoproduction, we learned that at high energies the total cross sections are dominated by the Pomeron exchange, which is responsible to the diffractive features of the data at small  $t$ . However, at low energies, meson exchanges or Reggeon exchanges are dominant over the Pomeron exchange and responsible to the bump structure of the total cross section near threshold. In  $\omega$  photoproduction, it is well-known that one-pion exchange is the most dominant process. In  $\rho$  photoproduction, however, the situation is not so clear. There are, in general, two models for the major production mechanism of  $\rho$  photoproduction at low energies. One is the  $\sigma$  meson exchange model<sup>13,14</sup> and the other is the  $f_2$  meson exchange model<sup>15–17</sup>.

The  $\sigma$  exchange model is motivated<sup>13</sup> by the observation that the  $\rho \rightarrow \pi\pi\gamma$  decay is much larger than the other radiative decays of the  $\rho$  meson such as  $\rho \rightarrow \pi\gamma$ . Therefore the role of  $2\pi$  exchanges is expected to be important in the production mechanism of  $\rho$  photoproduction. It is then assumed that the  $\pi\pi$  in the  $\pi\pi\gamma$  channel can be modeled as a  $\sigma$  meson such that the  $\sigma\rho\gamma$  vertex can be defined for calculating the  $\sigma$  exchange mechanism as illustrated in Fig. 1(b). In practice, the product of the coupling constants  $g_{\sigma\rho\gamma}g_{\sigma NN}$  of this tree-diagram is adjusted to fit the cross section data of  $\rho$  photoproduction at low energies. The parameters of the

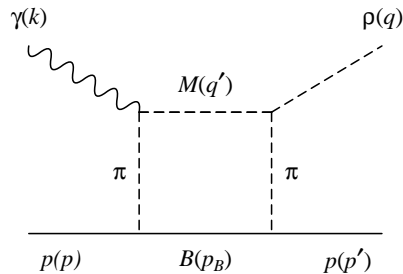


Figure 2.  $2\pi$  exchange in  $\rho$  photoproduction. The intermediate meson state ( $M$ ) includes  $\pi$  and  $\omega$ , and the baryon ( $B$ ) includes the nucleon.

$\sigma$  exchange model determined in this way are <sup>13, 14</sup>

$$M_\sigma = 0.5 \text{ GeV}, \quad g_{\sigma NN}^2/4\pi = 8.0, \quad g_{\sigma\rho\gamma} = 3.0. \quad (1)$$

The resulting  $\sigma$  mass parameter is close to the value  $M_\sigma = 0.55 \sim 0.66$  GeV of Bonn potential <sup>18</sup>. If we further take the value  $g_{\sigma NN}^2/4\pi = 8.3 \sim 10$  from Bonn potential, we then find that the resulting  $g_{\sigma\rho\gamma}$  is close to the values from the QCD sum rules,  $g_{\sigma\rho\gamma}(\text{QCDSR}) = 3.2 \pm 0.6$  <sup>19</sup> or  $2.2 \pm 0.4$  <sup>20</sup>. However such a large value of  $g_{\sigma\rho\gamma}$  overestimates the observed  $\rho \rightarrow \pi^0\pi^0\gamma$  decay width by two orders of magnitude <sup>21–24</sup>. If we accept the empirically estimated but model-dependent value of the SND experiment <sup>23</sup>,  $\text{BR}(\rho \rightarrow \sigma\gamma) = (1.9^{+0.9}_{-0.8} \pm 0.4) \times 10^{-5}$ , we get

$$|g_{\sigma\rho\gamma}| \approx 0.25. \quad (2)$$

This value is smaller than that of Eq. (1) by an order of magnitude. Therefore, the  $\sigma$  exchange model suffers from the big uncertainty of  $g_{\sigma\rho\gamma}$ . Furthermore, there is yet no clear particle identification of the  $\sigma$  meson and the use of  $\sigma$  exchange in defining  $NN$  potential has been seriously questioned. Thus it is possible that the  $\sigma$  exchange may not be the right major mechanism for  $\rho$  photoproduction.

Therefore, we take a different approach for  $\rho$  photoproduction <sup>17</sup> in this work. Here we consider the  $f_2$  exchange and two-pion exchange mechanisms. Instead of considering the radiative decay of the  $\rho$  through the  $\sigma$ , we consider the consequences of the strong  $\rho^0 \rightarrow \pi^+\pi^-$  decay which accounts for almost the entire decay width of the  $\rho$  meson. With the empirical value of the  $\rho$  meson decay width, one can define the  $\rho\pi\pi$  vertex which then leads naturally to the two-pion exchange mechanism illustrated in Fig. 2 with  $M = \pi$  in the intermediate state. Clearly, this two-pion exchange

mechanism is a part of the one-loop corrections discussed in Ref. 11 for  $\omega$  photoproduction. A more complete calculation of one-loop corrections to  $\rho$  photoproduction is accomplished in this work by including not only the intermediate  $\pi N$  state but also the intermediate  $\omega N$  state.

The  $f_2$  exchange model for  $\rho$  photoproduction was motivated by the analyses for  $pp$  elastic scattering<sup>25</sup>. In the study of  $pp$  scattering at low energies the secondary Regge trajectory is important, which is represented by the  $f$  trajectory. The idea of Pomeron- $f$  proportionality then had been used to model the Pomeron couplings from the  $f_2$  couplings<sup>26–28</sup> before the advent of the soft Pomeron model by Donnachie and Landshoff<sup>29</sup>. By considering the important role of the  $f$  trajectory in  $pp$  scattering, it is natural to consider the  $f_2$  exchange model for vector meson photoproduction. However, the  $f_2$  exchange model developed in Refs. 15, 16 for  $\rho$  photoproduction used the Pomeron- $f$  proportionality in the reverse direction. Namely, they assume that the structure of the  $f_2$  couplings is the same as that of the soft Pomeron exchange model. Thus the  $f_2$  tensor meson was treated as a  $C = +1$  isoscalar photon, i.e., a vector particle. In addition, the fit to the data is achieved by introducing an additional adjustable parameter to control the strength of the  $f_2$  coupling<sup>15</sup>. In this work, we elaborate an  $f_2$  exchange model starting from effective Lagrangians constructed by using the empirical information about the tensor properties of the  $f_2$  meson. The main objective of this work is to construct a model including this newly constructed  $f_2$  exchange amplitude and explicit two-pion exchange amplitude discussed above.

We now construct an  $f_2$  exchange model solely based on the tensor structure of the  $f_2$  meson. We will use the experimental data associated with the  $f_2$  meson, the tensor meson dominance, and vector meson dominance assumptions to fix the  $f_2$  coupling constants<sup>17,30,31</sup>, such that the strength of the resulting  $f_2$  exchange amplitude is completely fixed in this investigation. Following Refs. 32, 33, the effective Lagrangian accounting for the tensor structure of the  $f_2 NN$  interaction reads

$$\mathcal{L}_{f_2 NN} = -2i \frac{G_{f_2 NN}}{M_N} \bar{N} (\gamma_\mu \partial_\nu + \gamma_\nu \partial_\mu) N f^{\mu\nu} + 4 \frac{F_{f_2 NN}}{M_N} \partial_\mu \bar{N} \partial_\nu N f^{\mu\nu}, \quad (3)$$

where  $f^{\mu\nu}$  is the  $f_2$  meson field and  $M_N$  is the nucleon mass. The coupling constants were first estimated by using the dispersion relations in the analyses of the backward  $\pi N$  scattering<sup>32</sup> and the  $\pi\pi \rightarrow N\bar{N}$  partial-wave amplitudes. Here we use<sup>34</sup>

$$G_{f_2 NN}^2/4\pi = 2.2, \quad F_{f_2 NN} = 0. \quad (4)$$

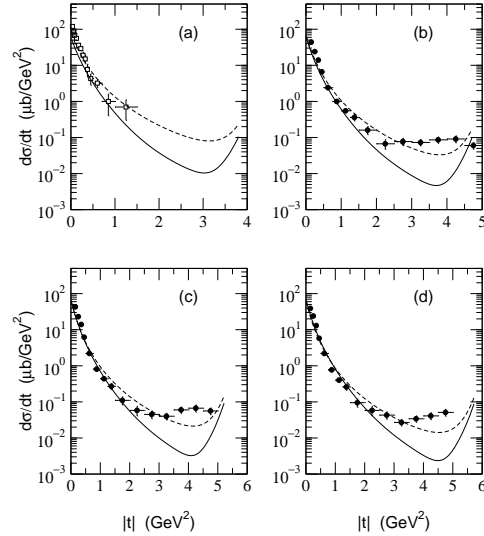


Figure 3. Differential cross sections of model (A) and (B) at  $E_\gamma = 3.55$  GeV. The dashed line is the result of model (A) and the solid line is that of model (B). Experimental data are from Ref. 2.

The most general form for the  $fV\gamma$  vertex satisfying gauge invariance reads<sup>30</sup>

$$\langle \gamma(k)V(k')|f_2 \rangle = \frac{1}{M_f} \epsilon^\kappa \epsilon'^\lambda f^{\mu\nu} A_{\kappa\lambda\mu\nu}^{fV\gamma}(k, k'), \quad (5)$$

where  $\epsilon$  and  $\epsilon'$  are the polarization vectors of the photon and the vector meson, respectively, and the form of  $A^{fV\gamma}$  can be found in Ref. 17. The tensor meson dominance together with the vector meson dominance constrain<sup>30</sup> the coupling constants of  $A^{fV\gamma}$ . The details on the  $f_2$  interactions and tensor meson dominance are given in Ref. 17.

In this work, we explore two models: model (A) includes the Pomeron,  $\sigma$ ,  $\pi$ ,  $\eta$  exchanges, and the  $s$ - and  $u$ -channel nucleon terms, while model (B) is constructed by replacing the  $\sigma$  exchange in model (A) by the  $f_2$  and  $2\pi$  exchanges. (See Figs. 1 and 2.) The full calculations of the  $\gamma p \rightarrow \rho^0 p$  differential cross sections from model (A) and (B) are compared in Fig. 3. From those figures, one may argue that model (B) is slightly better in small  $t$  region. However, it would be rather fair to say that the two models are comparable in reproducing the data. We therefore explore their differences in predicting the spin asymmetries, which are defined, e.g., in Ref. 35. The results for the single and double spin asymmetries are shown in Fig. 4 for

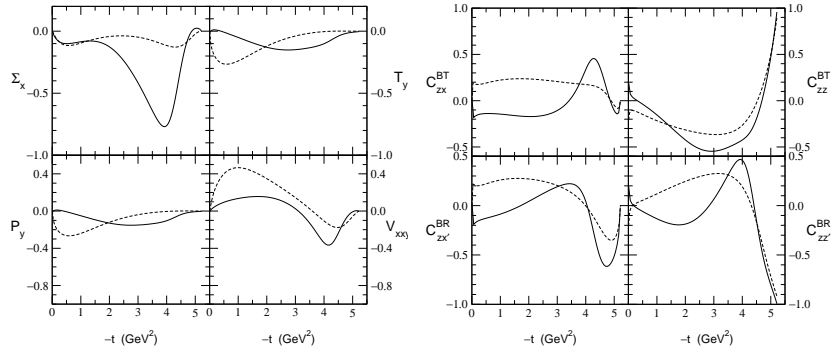


Figure 4. (left panel) Single spin asymmetries of model (A) and (B) at  $E_\gamma = 3.55$  GeV. (right panel) Double spin asymmetries  $C_{zx}^{BT}$ ,  $C_{zz}^{BT}$ ,  $C_{zx'}^{BR}$ , and  $C_{zz'}^{BR}$  of Model (A) and (B) at  $E_\gamma = 3.55$  GeV. Notations are the same as in Fig. 3.

$E_\gamma = 3.55$  GeV. Clearly the spin asymmetries would be useful to distinguish the two models and could be measured at the current experimental facilities. Of course our predictions are valid mainly in the small  $t$  region since the  $N^*$  excitations, which are expected to be important at large  $t$ <sup>8</sup>, are not included in this calculation. Therefore, measurements of such quantities at small  $t$  region should be crucial to understand the main non-resonant production mechanisms of  $\rho$  photoproduction at low energies.

Finally let us mention about the role of the  $f_2$  exchange in  $\phi$  photoproduction. In this case, we can consider the exchanges of the  $f_2(1270)$  and  $f_2'(1525)$  mesons. However such exchanges are expected to be negligible *if* the  $f_2$  and  $f_2'$  mixing is close to the ideal mixing. This is because the ideal mixing makes the  $f_2\phi\gamma$  and  $f_2'NN$  couplings vanish, although  $f_2NN$  and  $f_2'\phi\gamma$  do not. Since the amplitude of this process contains  $g_{f_2\phi\gamma}G_{f_2NN}$  or  $g_{f_2'\phi\gamma}G_{f_2'NN}$ , its contribution is expected to be small if the  $f_2$ - $f_2'$  mixing is close to the ideal mixing.

### Acknowledgments

Y.O. was supported by Korea Research Foundation Grant (KRF-2002-015-CP0074) and T.-S.H.L. was supported by U.S. DOE Nuclear Physics Division Contract No. W-31-109-ENG-38.

### References

1. CLAS Collaboration, E. Anciant *et al.*, Phys. Rev. Lett. **85**, 4682 (2000); K. Lukashin *et al.*, Phys. Rev. C **63**, 065205 (2001), **64**, 059901(E) (2001).

2. CLAS Collaboration, M. Battaglieri *et al.*, Phys. Rev. Lett. **87**, 172002 (2001).
3. CLAS Collaboration, M. Battaglieri *et al.*, Phys. Rev. Lett. **90**, 022002 (2003).
4. J. Ajaka *et al.*, in *Proceedings of 14th International Spin Physics Symposium*, edited by K. Hatanaka *et al.*, (AIP Conf. Proc. **570**, 2001), p. 198.
5. T. Nakano, in *Proceedings of 14th International Spin Physics Symposium*, edited by K. Hatanaka *et al.*, (AIP Conf. Proc. **570**, 2001), p. 189.
6. T. Mibe, in these proceedings.
7. S. Capstick and W. Roberts, Prog. Part. Nucl. Phys. **45**, S241 (2000).
8. Y. Oh, A. I. Titov, and T.-S. H. Lee, Phys. Rev. C **63**, 025201 (2001).
9. Q. Zhao, Z. Li, and C. Bennhold, Phys. Rev. C **58**, 2393 (1998).
10. A. Titov and T.-S. H. Lee, Phys. Rev. C **67**, 065205 (2003).
11. Y. Oh and T.-S. H. Lee, Phys. Rev. C **66**, 045201 (2002); Nucl. Phys. A **721**, 743 (2003).
12. G. Penner and U. Mosel, Phys. Rev. C **66**, 055211 (2002).
13. B. Friman and M. Soyeur, Nucl. Phys. A **600**, 477 (1996).
14. Y. Oh, A. I. Titov, and T.-S. H. Lee, nucl-th/0004055, in *NSTAR2000 Workshop*, edited by V. Burkert *et al.*, (World Scientific, Singapore, 2000), p. 255.
15. J.-M. Laget, Phys. Lett. B **489**, 313 (2000).
16. N. I. Kochelev and V. Vento, Phys. Lett. B **515**, 375 (2001); **541**, 281 (2002).
17. Y. Oh and T.-S. H. Lee, nucl-th/0306033.
18. R. Machleidt, K. Holinde, and C. Elster, Phys. Rep. **149**, 1 (1987).
19. A. Gokalp and O. Yilmaz, Phys. Rev. D **64**, 034012 (2001).
20. T. M. Aliev, A. Özpıneci, and M. Savcı, Phys. Rev. D **65**, 076004 (2002).
21. A. Gokalp and O. Yilmaz, Phys. Lett. B **508**, 25 (2001).
22. A. Bramon, R. Escribano, J. L. Lucio M., and M. Napsuciale, Phys. Lett. B **517**, 345 (2001).
23. SND Collaboration, M. N. Achasov *et al.*, Phys. Lett. B **537**, 201 (2002).
24. Y. Oh and H. Kim, hep-ph/0307286.
25. A. Donnachie and P. V. Landshoff, Phys. Lett. B **296**, 227 (1992).
26. P. G. O. Freund, Phys. Lett. **2**, 136 (1962); Nuovo Cimento **5A**, 9 (1971).
27. R. Carlitz, M. B. Green, and A. Zee, Phys. Rev. Lett. **26**, 1515 (1971).
28. Yu. N. Kafiev and V. V. Serebryakov, Nucl. Phys. B **52**, 141 (1973).
29. A. Donnachie and P. V. Landshoff, Nucl. Phys. B **244**, 322 (1984).
30. B. Renner, Phys. Lett. **33B**, 599 (1970); Nucl. Phys. B **30**, 634 (1971).
31. K. Raman, Phys. Rev. D **3**, 2900 (1971).
32. H. Goldberg, Phys. Rev. **171**, 1485 (1968).
33. H. Pilkuhn *et al.*, Nucl. Phys. B **65**, 460 (1973).
34. N. Hedegaard-Jensen, Nucl. Phys. B **119**, 27 (1977); E. Borie and F. Kaiser, *ibid.* **126**, 173 (1977).
35. A. I. Titov, Y. Oh, S. N. Yang, and T. Morii, Phys. Rev. C **58**, 2429 (1998).